

# All-Photonic Multifunctional Molecular Logic Device

Joakim Andréasson,<sup>\*,†</sup> Uwe Pischel,<sup>\*,‡</sup> Stephen D. Straight,<sup>§</sup> Thomas A. Moore,<sup>§</sup> Ana L. Moore,<sup>§</sup> and Devens Gust<sup>\*,§</sup>

<sup>†</sup>Department of Chemical and Biological Engineering, Physical Chemistry, Chalmers University of Technology, SE-412 96 Göteborg, Sweden

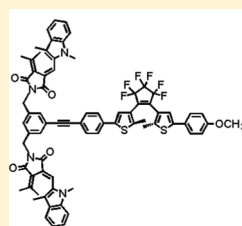
<sup>‡</sup>Center for Research in Sustainable Chemistry and Department of Chemical Engineering, Physical Chemistry, and Organic Chemistry, University of Huelva, Campus de El Carmen s/n, E-21071 Huelva, Spain

<sup>§</sup>Department of Chemistry and Biochemistry, Arizona State University, Tempe, Arizona 85287-1604, United States

**S** Supporting Information

**ABSTRACT:** Photochromes are photoswitchable, bistable chromophores which, like transistors, can implement binary logic operations. When several photochromes are combined in one molecule, interactions between them such as energy and electron transfer allow design of simple Boolean logic gates and more complex logic devices with all-photonic inputs and outputs. Selective isomerization of individual photochromes can be achieved using light of different wavelengths, and logic outputs can employ absorption and emission properties at different

wavelengths, thus allowing a single molecular species to perform several different functions, even simultaneously. Here, we report a molecule consisting of three linked photochromes that can be configured as AND, XOR, INH, half-adder, half-subtractor, multiplexer, demultiplexer, encoder, decoder, keypad lock, and logically reversible transfer gate logic devices, all with a common initial state. The system demonstrates the advantages of light-responsive molecules as multifunctional, reconfigurable nanoscale logic devices that represent an approach to true molecular information processing units.



All-photonic	✓	Encoder	✓
Half-adder	✓	Decoder	✓
Half-subtractor	✓	Keypad lock	✓
Multiplexer	✓	Reversible logic	✓
Demultiplexer	✓		

## INTRODUCTION

The beguiling idea that molecules can manipulate and process information using logic,<sup>1</sup> as do electronic computers and human brains, has spawned numerous studies of molecule-based systems that perform not only as simple logic gates but also as more complex devices<sup>2–4</sup> such as adders and subtractors,<sup>5–7</sup> multiplexers/demultiplexers,<sup>8–10</sup> encoders/decoders,<sup>11,12</sup> keypad locks,<sup>13–17</sup> and multivalued logic devices.<sup>18,19</sup> In recent years, such decision-making molecular systems<sup>20</sup> have been explored in clever applications taking advantage of binary and multivalued information processing<sup>18,19</sup> for multiparameter chemosensing,<sup>21</sup> pro-drug activation,<sup>22,23</sup> medical diagnostics,<sup>24,25</sup> object labeling,<sup>26</sup> data storage,<sup>27,28</sup> and smart materials and surfaces.<sup>29–32</sup>

Molecular computing, which requires more than a single logic function/device, has been critically discussed in recent years.<sup>4,33,34</sup> One of the foremost problems is the physical integration of many logic gates in arrays in order to achieve functional complexity beyond basic logic gates such as AND, OR, NOR, NAND, XOR, INH, etc. This would require efficient wiring (concatenation) of simple logic switches. Only a few proof-of-principle examples of such concatenation are known in the literature.<sup>29,35–42</sup> One approach to circumvent this problem is functional integration.<sup>43</sup> This means that a unimolecular system can mimic a complex logic circuit, composed of various logic gates, without the necessity of representing each logic gate by a different structural

feature. The complex logic devices mentioned above are examples of this approach. For example, a molecular half-adder is a combination of AND and XOR logic gate functions in the same molecule.

Many of the molecular logic systems that have been described use chemicals as inputs and optical as well as chemical signals as outputs.<sup>14,38</sup> However, the use of photons for both inputs and outputs offers several advantages.<sup>44</sup> First, due to the physical equality of input and output, i.e., an all-photonic operation, one barrier for the concatenation of logic devices is removed. Also, light does not require physical access, allowing monolithic structures containing many individual logic elements. This is a potential advantage for transferring molecular logic devices from solution operation to the solid phase in the future. Light does not lead to the buildup of waste products, thus in principle allowing nearly infinite cycling of the system (although this has not been achieved yet in practice). Optical input signals can be delivered by remote control and as pulses, even on the subpicosecond time scale, permitting rapid cycling. Importantly, different chromophores in the same molecule interact differently with light of different wavelengths. Moreover, a single substance can perform several logic operations with the same set of inputs, depending

**Received:** April 14, 2011

**Published:** May 12, 2011

upon the readout selected, and may be reconfigured for different operations simply by changing the input wavelengths, output wavelengths, or initial state.

We report here a photochromic triad acting as a unimolecular, multifunctional, and reconfigurable logic system that performs the functions of the following devices: AND, XOR (exclusive OR), INH (inhibit), half-adder, half-subtractor, multiplexer, demultiplexer, encoder, decoder, keypad lock, and logically reversible transfer gate. Uniquely, all operations use a common initial state, and the majority (including the half-adder and half-subtractor) share the same two inputs, differing only in the choice of the optical output signal. This not only allows parallel logic operations with the same set of inputs but also makes switching (reconfiguration)<sup>45,46</sup> among the various logic operations extremely rapid and convenient. The thereby achieved level of functional integration through implementation of logic gate arrays<sup>47</sup> without the need of physical gate-to-gate connections is unprecedented.<sup>48–50</sup> Additionally, the triad can be reset by a universal optical signal, independent of the preceding input combination/logic operation.

## EXPERIMENTAL SECTION

Distilled 2-methyltetrahydrofuran was the solvent for spectroscopic measurements. The samples were degassed by six freeze–pump–thaw cycles to a final pressure of approximately  $10^{-5}$  Torr. The absorption measurements were performed using a CARY 4000 UV/vis spectrometer. A SPEX Fluorolog  $\tau 2$  was used for the emission measurements. After exposure to the different input combinations, the absorbance and emission were monitored separately using the instruments mentioned above. The sample concentration was  $\sim 2.5 \times 10^{-5}$  M. The 397 nm light, the broad band green light, and the red light were generated by a 1000 W Xe/Hg lamp at 450 W equipped with a hot mirror ( $A = 1.8$  at 900 nm) to reduce the IR intensity. A 397 nm interference filter was used for the 397 nm light, a VG 9 glass filter ( $A < 1.5$  between 460 and 590 nm) was used for the broad band green light, and a long-pass filter ( $A > 1.5$  at  $\lambda < 615$  nm) was used for the red light. The resulting light power densities were  $\sim 1.6$ ,  $\sim 9$ , and  $\sim 50$  mW/cm<sup>2</sup> for the 397 nm light, the green light, and the red light, respectively. The 302 and 366 nm UV light were generated by VVP hand-held UV lamps (models UVM-57 and UVGL-25, respectively, each with a power density of 1.5 mW/cm<sup>2</sup> at the sample). The total sample volume was ca. 3 mL. When using the 397 nm light, the broad band green light, and the red light, only one-third of the sample volume was exposed to the light at any given time, whereas the whole sample volume was exposed to the 302 and 366 nm light. The samples were stirred continuously during all irradiation processes.

## RESULTS AND DISCUSSION

**The Molecule and Its Photochemistry.** Molecular triad FG-DTE<sup>11</sup> (Figure 1a) consists of three covalently linked photochromic chromophores: a dithienylethene (DTE) and two fulgimides (FG). Using different wavelengths, the two kinds of photochromes may be photoisomerized independently between open forms (DTEo, FGo; top half of Figure 1a) and closed forms (DTEc, FGc; lower half of Figure 1a). Thus, the molecule may exist in six constitutionally isomeric forms (stereoisomers exist but are not relevant for the operations discussed here). For this study, only the four isomers in which the two identical fulgimides are in the same form (open or closed) are relevant. These four isomers are labeled FGo-DTEo, FGc-DTEo, FGo-DTEc, and FGc-DTEc (Figure 1).

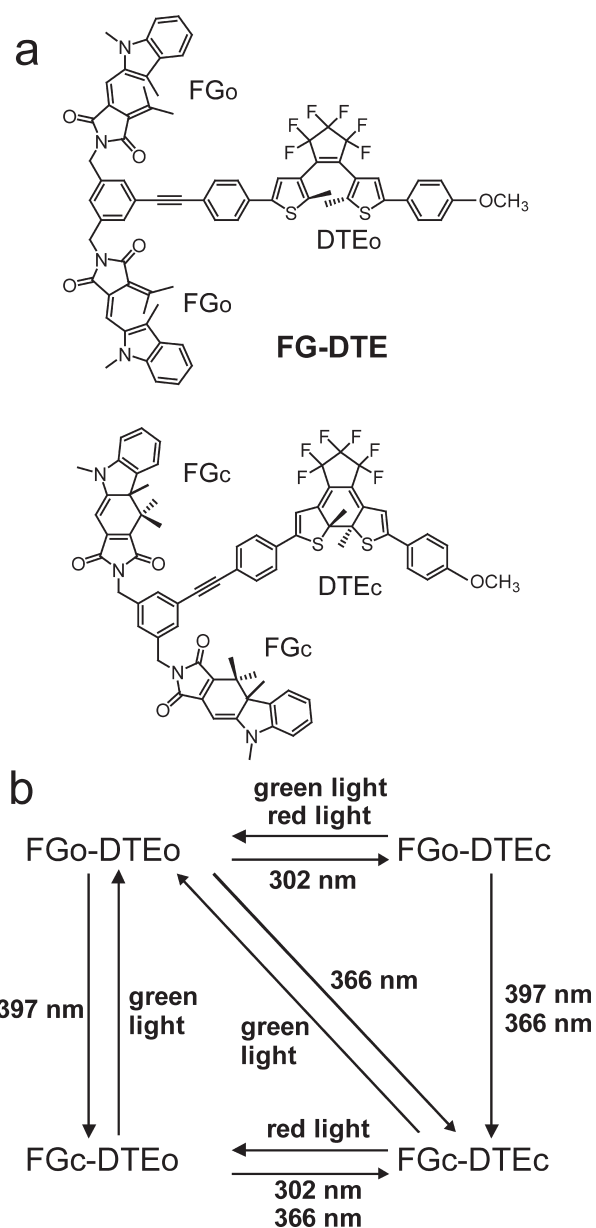


**Figure 1.** Structure and photochemistry of FG-DTE. (a) The upper structure, FGo-DTEo, shows the molecule with all three photochromes in the open forms, which have no absorption in the visible. In the lower structure, FGc-DTEc, all three photochromes are in the closed forms. As discussed in the text, various combinations of open and closed forms can exist. (b) Photochemical interconversions among the four photoisomeric structures relevant for this work. The conditions for generating the light beams are given in the Experimental Section, and the photoisomerization rates are described in the Supporting Information.

Each isomer has a unique spectral signature (Figure 2), allowing conversion of an isomer mixture in a solvent such as 2-methyltetrahydrofuran into a solution highly enriched in any of the four forms (Figure 1b). For example, the thermally most stable form, FGo-DTEo, does not absorb beyond 450 nm. If it is irradiated at 397 nm, where absorption is due almost entirely to FGo (see model compounds, Supporting Information, Figures S1 and S2), isomerization to a photostationary state consisting mainly of FGc-DTEo occurs. The spectrum of this isomer (Figure 2) features weak absorption around 397 nm and a new absorption at

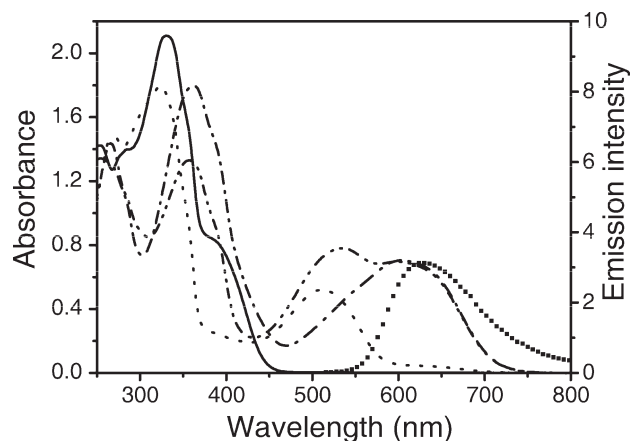


**Figure 2.** Absorption and emission spectra of different forms of FG-DTE. Solid line, thermally stable FGo-DTEo; dotted line: FGc-DTEo; dash-dot, FGo-DTEc; dash-dot-dot, FGc-DTEc. Also shown is the emission from FGc in the FGo-DTEo form of the molecule (squares). Note the pronounced overlap between the emission of FGc and the absorption of DTEc, which is favorable for energy transfer.

511 nm. The new band is due to FGc, which fluoresces with a maximum at 624 nm. Green light irradiation ( $460 < \lambda < 590$  nm) converts FGc-DTEo back to FGo-DTEo. If the solution of FGo-DTEo is instead irradiated at 302 nm, where most of the absorption is due to DTEo, the sample is isomerized to a photostationary state containing mainly FGo-DTEc. The absorption spectrum (Figure 2) of FGo-DTEc features a new band at 604 nm due to DTEc, which is not significantly fluorescent. Similar interconversions among all four isomers may be achieved with light of various wavelengths (Figure 1b). The isomerization conditions and kinetics are presented in the Supporting Information, and a more detailed description of the synthesis and photochemistry of the molecule, including its excellent photo- and thermal stability, has appeared.<sup>11</sup> Importantly, isomer FGc-DTEc is not fluorescent, even though it features fulgimides in the closed form. This is because the molecule was designed so that singlet excitation energy is rapidly ( $\tau < 5$  ps) transferred from FGc to DTEc, thus quenching the fluorescence.<sup>11</sup> As will be explained below, this feature, achievable only in a covalently linked system, is vital for several logic functions. At the same time, the electronic coupling is sufficiently weak to preserve the identity of the individual chromophores, allowing for the selective isomerization of the different photochromes.

**Molecular Logic.** The photochemistry briefly described above forms the basis for molecular logic. Irradiation into the various absorption bands constitutes device inputs. Each input causes photoisomerization, which comprises the switching operation central to binary logic. After photoisomerization, the molecule remains in the selected state, recording the result of the inputs after they are turned off and allowing subsequent readout. The choice of readout (absorbance at a particular wavelength or emission) selects the logic operation performed. Inputs and outputs were achieved using conventional instrumentation (see Experimental Section).

**Binary Arithmetic.** Binary addition and subtraction can be achieved by combinations of AND, XOR, and INH logic gates. Many molecular gates have been reported, and molecule-based systems that combine these functions are approaches to molecular

**Table 1.** Truth Tables for Binary Arithmetic<sup>a</sup>

inputs		outputs			
<i>a</i> (397 nm)	<i>b</i> (302 nm)	AND gate (A 535 nm)	XOR gate ( $ \Delta A $ 393 nm)	INH1 gate (A 393 nm)	INH2 gate (Em 624 nm)
0	0	0	0	0	0
1	0	0	1	0	1
0	1	0	1	1	0
1	1	1	0	0	0

<sup>a</sup> The last four columns give the outputs for each of the basic logic gates elicited by the various input combinations. The outputs for the half-adder are given by a combination of the AND and XOR outputs, whereas those for a half-subtractor are given by those of the XOR plus INH1 or INH2.

calculators, or “moleculators”.<sup>5,6,51,52</sup> The FG-DTE triad is the first example of a molecular species capable of performing all these functions using only two inputs: irradiation at 397 nm (input *a*) or at 302 nm (input *b*). Furthermore, all operations share a common initial state, FGo-DTEo, to which any other state may be reset by a universal operation: green light irradiation. This implies that it is possible to perform addition and subtraction in parallel, simply by monitoring the outputs at wavelengths where the spectral changes correspond to AND, XOR, and INH logic. The first two columns in Table 1 show the possible combinations with the inputs on (1) or off (0), together with the corresponding outputs of the relevant logic gates shown in columns 3–6.

We will first illustrate the simple logic gate functions of FG-DTE. The logic of the AND gate is that the output remains off unless both inputs are turned on. A solution of FG-DTE functions as an AND gate with the absorbance at 535 nm as the output (Figure 3a). When the absorbance increases above a threshold value, indicated by a dashed line in Figure 3, the output switches from 0 to 1. This occurs only when both inputs are applied. Chemically, this happens because the two input wavelengths, applied together or in any sequence, convert FGo-DTEo to FGc-DTEc (Figure 1b), which is the only isomer having the requisite strong absorbance at 535 nm (Figure 2). Note that although switches in binary arithmetic theoretically may have values of only 0 or 1, not only this but all real devices including transistors function via a threshold. The tops of the black bars in Figure 3 show the actual spectrometer traces for the measurements; the signal noise is barely apparent.

In the XOR gate, the output is on only if one or the other but not both inputs are applied. A solution of FG-DTE functions as an XOR gate when the absolute value (modulus) of the absorption change at 393 nm,  $|\Delta A|$ , is monitored. As seen in Figure 2, the absorbances of FGo-DTEo and FGc-DTEc are essentially identical at this wavelength, but the absorbance of the other two isomers is either much higher or much lower. It is evident from Figure 3b that  $|\Delta A|$  is above the threshold only when a single input is applied, but not both, as required for XOR. Reading  $|\Delta A|$  as an output requires an additional data processing step. It has been suggested by other authors that this can be implemented by the integration of circuitry into the spectrometer used in the readout operation.<sup>38,52</sup>

The molecule can function as two complementary INH gates (INH1 and INH2), each responding to a different input. As shown in Table 1, INH gates give an output of 1 only when one

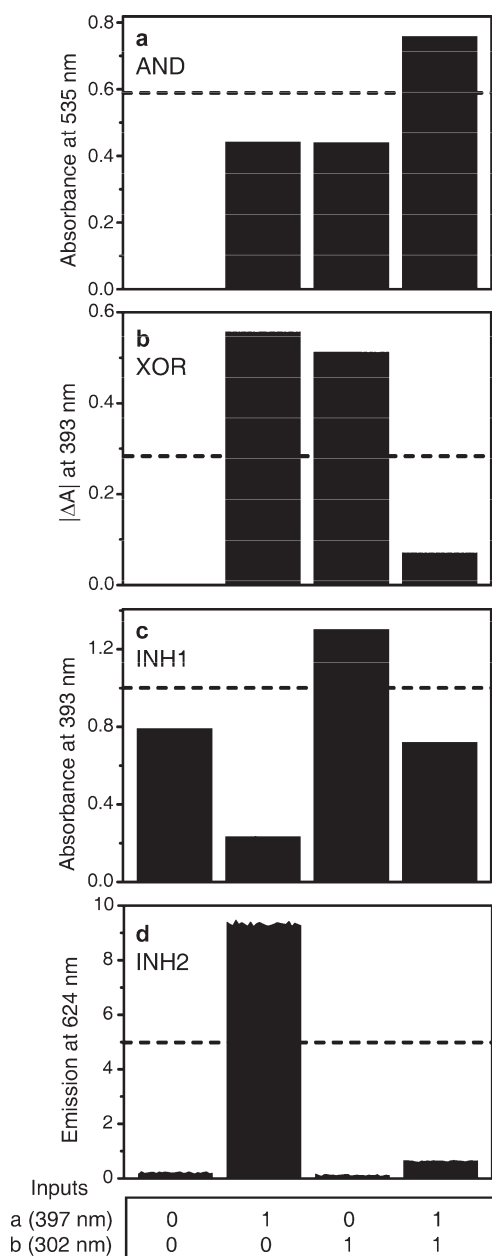


**Figure 3.** Performance of the gate functions for the half adder (AND and XOR) and the half-subtractor (XOR, INH1, and INH2). The input combinations (0 = off, 1 = on) for all gates are shown at the bottom of the figure. The bar graphs show the nature of the output for each gate as the Y-axis label and the performance of FG-DTE as amplitude bars relative to a threshold (dashed line). The top of each bar shows the actual experimental data and associated noise. Noise is essentially indistinguishable except for INH2.

particular input (not the other or both) is applied; i.e., one of the inputs inhibits the gate from responding to the other. With the absorbance at 393 nm as an output, it can be seen from Figure 2 that this will be above the threshold only in FGc-DTEc, where both chromophores contribute to the absorption. As shown in Figure 1b and Figure 3c, INH1 is switched to the on-state only upon application of input *b* (302 nm). The second inhibit gate, INH2, is implemented by monitoring fluorescence at 624 nm. Fluorescence occurs only in FGc-DTEo, where FGc fluorescence

is not quenched by the closed form of DTE. Input *a* at 397 nm produces this state (Figures 2 and 3d).

The simple logic gate functions described above are combined to produce more complex logic operations. Combining the AND and XOR gates, which use the same inputs, produces a half-adder. The half-adder adds two binary digits represented by the two inputs, each of which represents a 0 (off) or 1 (on). The readout of XOR represents the sum digit, and that of AND the carry digit. If neither input is on, both gates read out 0. This gives the binary sum 00, representing the decimal sum of  $0 + 0 = 0$ . If either input is turned on, AND reports a 0 whereas XOR reports a 1. Now, the binary sum reads 01 ( $0 + 1 = 1$  in the decimal notation). If both inputs are on, XOR reads out 0, and the AND gate delivers an on output. This concludes the truth table for the half-adder, as the binary output combination 10 represents the decimal 2 ( $1 + 1 = 2$ ).

The half-subtractor results from the combination of the XOR and INH1 gates responding to the same inputs. The XOR represents the difference, and the INH1 the borrow output. If input  $a = 1$  and input  $b = 0$ , then  $a - b = 1 - 0 = 1$ . Figure 3 shows that in this case, the XOR gate gives a difference of 1 and the INH1 gate shows that nothing (0) was borrowed. If instead input  $a = 0$  and input  $b = 1$ , then  $a - b = 0 - 1 = -1$ . Now, the XOR gate gives a difference of 1 and the INH1 gate shows that 1 was borrowed. Finally, when both inputs are on or off,  $1 - 1 = 0 - 0 = 0$  applies, as is indicated by a 0 output from both gates. If XOR and INH2 are used instead, a half-subtractor calculating  $b - a$  results; i.e., the order of subtrahend and minuend is conveniently switched by monitoring the output at two different wavelengths.<sup>53,54</sup>

**Multiplexer.** Molecular logic systems can perform non-arithmetic functions as well. Digital multiplexers are analogous to mechanical rotary switches that connect any one of several inputs to the output. The FG-DTE molecule can function as a 2:1 multiplexer (MUX, Figure 4). As shown in Table 2, the multiplexer has two data inputs, In1 (397 nm light) and In2 (red light, >615 nm). A third input, the selector input (Sel, 366 nm light) is applied to the initial state (FGo-DTEo) before the data inputs and determines which data input's state will be transmitted to the output (emission at 624 nm). When Sel is off, the state of In1 is directly transferred to the output, and the state of In2 is ignored, whereas if Sel is on, the output instead reports the state of In2 and ignores the state of In1. The multiplexer is reset from any triad state to the FGo-DTEo initial state using green light. Illumination conditions are reported in the Supporting Information.

When Sel is off (Figure 4a), the triad remains as FGo-DTEo prior to any application of In1 or In2. In1 converts the sample to FGc-DTEo (Figure 1b), which fluoresces, giving an output signal (output = 1). Alternatively, In2 has no effect, and the molecule remains in the non-fluorescent FGo-DTEo state (output = 0). When both inputs are applied, FGc-DTEo is again produced by the action of In1, and as the red light (In2) has no effect on either FGo-DTEo or FGc-DTEo, fluorescence is observed (output = 1). Hence, the output reflects the state of In1, regardless of the state of In2. When Sel (366 nm) is applied both FGo and DTEo isomerize to the closed forms, converting the triad to FGc-DTEc (Figure 4b). This form is not fluorescent due to energy transfer quenching of the FGc excited state by DTEc: the output remains off. If In1 is then turned on, the 397 nm light has no effect as FG is already in the closed form, and the output is off. On the other hand, if In2 is turned on, the red light isomerizes DTEc to DTEo giving the fluorescent FGc-DTEo, so that the output turns on. Therefore, when Sel has been applied, the output reflects the state of In2, regardless of In1, as required for the multiplexer.

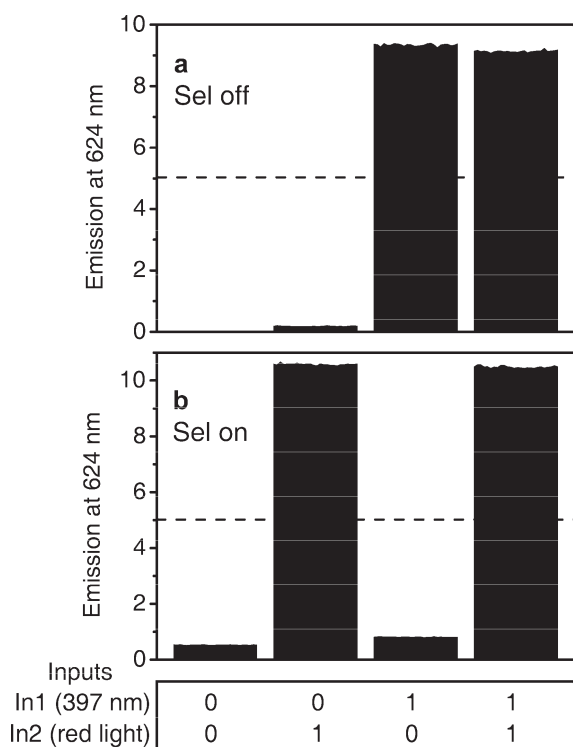


**Figure 4.** Performance of FG-DTE as a 2:1 multiplexer. The input combinations (0 = off, 1 = on) are shown at the bottom of the figure. The experimental response levels for the output of FG-DTE (emission at 624 nm) with Sel off and on are shown in panels a and b, respectively. The noise level is apparent at the tops of the bars.

**Table 2. Truth Table for the 2:1 Multiplexer**

In1 (397 nm)	In2 (red light)	Sel (366 nm)	output (Em 624 nm)
0	0	0	0
0	1	0	0
1	0	0	1
1	1	0	1
0	0	1	0
0	1	1	1
1	0	1	0
1	1	1	1

**Demultiplexer.** Once two signals have been multiplexed into one output, they can be separated again using a demultiplexer (DMUX). This allows multiple signals to be combined in the MUX, transmitted on the same data line, and individually recovered again by the DMUX at the other end of the line. The FG-DTE triad can function as a 1:2 digital demultiplexer, reversing the effect of a 2:1 digital multiplexer like the one described above. A 1:2 demultiplexer thus has one data input containing the entangled data from the upstream MUX; i.e., the output from the MUX serves as the input (In) for the DMUX. The data bits are now disentangled in the DMUX to either output 1 (O1) or output 2 (O2), depending on the state of a second input; the address input (Ad). The truth table is shown in Table 3, and the function is shown in Figure 5. The initial state when operated as the DMUX is again FGo-DTEo, as for all

**Table 3. Truth Table for the 1:2 Demultiplexer**

In (397 nm)	Ad (302 nm)	O1 (Em 624 nm)	O2 (A 535 nm)
0	0	0	0
1	0	1	0
0	1	0	0
1	1	0	1

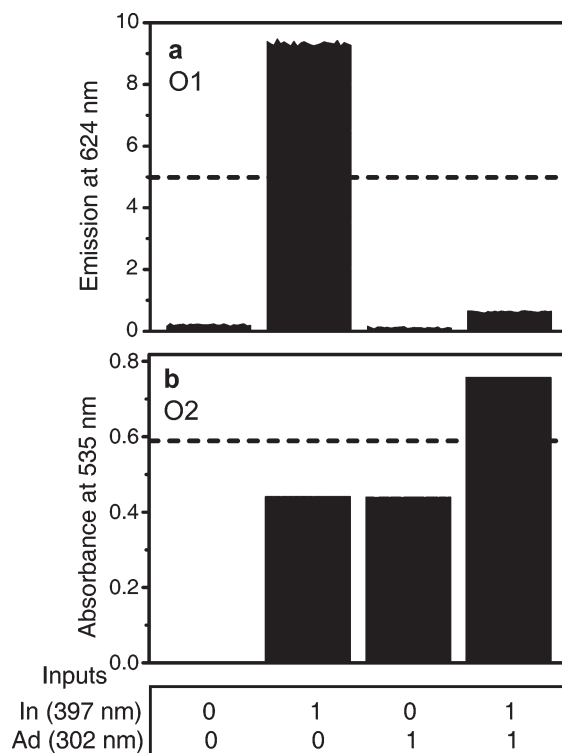


**Figure 5.** Performance of FG-DTE as a 1:2 demultiplexer. The input combinations (0 = off, 1 = on) are shown at the bottom of the figure. The experimental response levels for the outputs of FG-DTE (emission at 624 nm and absorbance at 535 nm) are shown in panels a and b, respectively. The noise level is apparent at the tops of the bars.

herein described logic devices. The data input (In) is light at 397 nm, and 302 nm serves as the address (Ad) input that determines to which output the input data are sent. When Ad is off, the input signal In is directed to output O1 (emission at 624 nm, Figure 5a), and when Ad is on, the output appears at output O2 (absorbance at 535 nm, Figure 5b). Chemically, when Ad is off, an on state of the input (397 nm) converts the non-fluorescent, colorless FGo-DTEo to FGc-DTEo, where the fluorescence of FGc at 624 nm gives an on output to O1. The absorbance at 535 nm is still below the threshold level, and output O2 remains off. Thus, the output of DMUX directs the on or off state of data input In to output O1. When Ad (302 nm) is applied, the triad isomerizes to the nonfluorescent FGo-DTEc form, and both outputs are off with no input. When the 397 nm input is now applied, FGc-DTEc is formed, giving an absorbance at 535 nm above the threshold level, whereas the emission intensity is still low due to energy-transfer fluorescence quenching. The output is shunted to O2, completing the function of the DMUX.

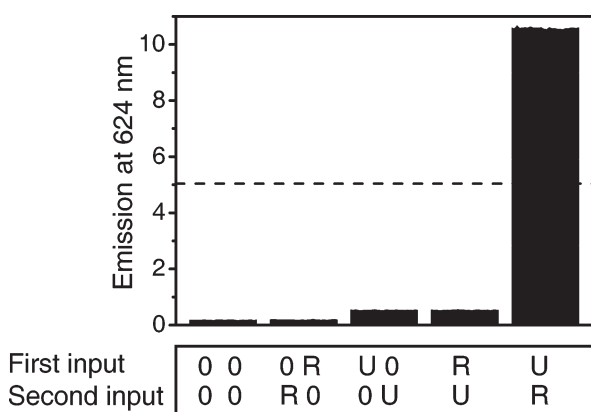


**Figure 6.** FG-DTE molecule as a keypad lock. The inputs are red light (R, >615 nm) and UV light (U, 366 nm). An output (fluorescence at 624 nm) greater than the threshold (dashed line) is produced only when the inputs are applied in the correct order (U, then R), as shown in the bar graph.

**Keypad Lock.** All functions described so far are so-called combinational logic functions, as the state of the output is determined only by the input combination without regard to the order of their application. In contrast to this behavior are the sequential logic functions, where the output signal switches on only when the correct inputs are applied *in the correct order*.<sup>55–57</sup> This implies a memory function of the device. The sequential logic differs fundamentally from the combinational logic gates, in which either input may be applied first. The keypad lock is one example of a sequential logic device, as the lock opens (output switches on) only upon receiving the correct sequence of inputs. With one exception,<sup>17</sup> previously reported molecular keypad locks have employed chemical, rather than photonic inputs.<sup>15–17,57,58</sup> As a keypad lock, FG-DTE has two inputs, each of which may be in either the on or off state, giving rise to eight possible two-digit order-sensitive codes. As shown in Figure 6, the inputs are red light (R, >615 nm) and UV light (U, 366 nm). Green light resets the triad to the initial state, which again is FGo-DTEo. The output is fluorescence of FGc at 624 nm. Red light alone does not affect the sample at all, whereas UV light converts it to the non-fluorescent FGc-DTEc (Figure 1b). Thus, none of the first six sets of ordered inputs shown in Figure 6 results in an output. Likewise, red light followed by UV light generates the non-fluorescent FGc-DTEc. However, UV light as the first input prepares FGc-DTEc, and a subsequent application of red light yields FGc-DTEo (see Figure 1b), which fluoresces: the lock opens. It is noteworthy that the described sequential switching is characterized by a high dynamic range (fluorescence enhancement factor for on switching is  $\geq 20$ ), enabling unambiguous identification of the “lock open” situation.

**Dual Transfer Gates—Reversible Logic.** Transfer gates simply transfer the state of an input to that of an output with no logical change (0 becomes 0, 1 becomes 1). They are useful in systems of concatenated logic gates for the conversion of the output of one gate into the input of a second. Concatenation of gates is necessary if molecular logic is to be used to carry out complicated computational operations.<sup>29,35–42</sup> The FG-DTE system can be configured as two transfer gates, TN1 and TN2 (Figure 7). Furthermore, these two gates together comprise a logically reversible logic system, wherein each combination of inputs gives a unique output. This would not have been the case if

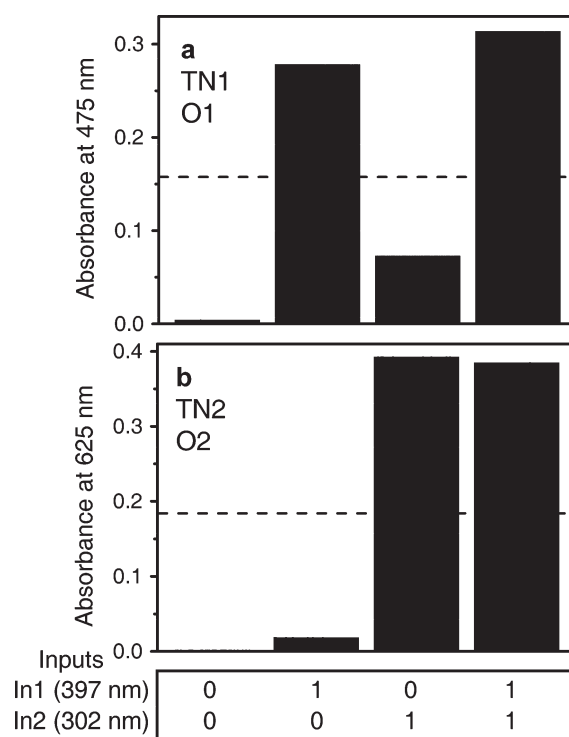


**Figure 7.** Performance as transfer gates. The various input states for the two transfer gates are shown at the bottom of the Figure, and the bar graphs show the experimental response of the two transfer gates (absorbance at 475 and 625 nm) to the inputs, relative to the indicated threshold values (dashed lines).

**Table 4. Truth Table for the Transfer Gates**

In1 (397 nm)	In2 (302 nm)	O1 (A 475 nm)	O2 (A 625 nm)
0	0	0	0
1	0	1	0
0	1	0	1
1	1	1	1

for example TN1 alone were used to generate only O1. It is clearly seen in Table 4 that two different input combinations (00 and 01) generate an off (0) response at output O1, whereas both 10 and 11 generate an on (1) response. For output O2 a related situation applies (see Table 4).

Hence, information would be lost in a logic gate processing with either output O1 alone or O2 alone. Reversible logic avoids this issue, because each input vector is represented by a non-repeated output vector. This is becoming of interest in electronic computers and may have importance in molecular logic as well.<sup>54,59</sup> When FG-DTE is used as a reversible logic device, the inputs are light at 397 nm (In1) and light at 302 nm (In2), the outputs are absorbance at 475 nm (O1) and 625 nm (O2), the initial state is FGo-DTEo, and the reset is green light. Chemically, In1 isomerizes FGo to FGc, absorbing strongly at 475 nm (O1), whereas 302 nm isomerizes DTEo to DTEc with strong absorption at 625 nm (O2). The function is shown in Figure 7, and it is clear that O1 tracks the state of In1 and O2 tracks In2. This is a direct consequence of the independent photochromic switching

of FG and DTE entities in the triad by application of the light inputs at the particular wavelengths. In addition, each unique input combination gives a unique output combination, showing that logical reversibility is achieved.

**Encoder and Decoder.** An encoder compresses digital information for transmission or storage, and a decoder recovers the information in its original form. The FG-DTE system performs both as a single bit 4-to-2 encoder and 2-to-4 decoder, where respectively, numbers in base-10 are translated into binary numbers, and vice versa. This function of the molecule has been previously described.<sup>11</sup> Briefly, the encoder inputs are light at four different wavelengths, 460, 397, 302, and 366 nm, and the outputs are absorbance at 475 and 625 nm. When acting as a decoder, the inputs are light at 397 and 302 nm, and the outputs are absorbance at 393 and 535 nm, transmittance at 535 nm, and fluorescence at 624 nm. The initial state for both functions is FGo-DTEo.

## CONCLUSIONS

The FG-DTE system of four photonically interconvertible isomers can thus be operated as any of 13 digital logic devices. Switching is achieved with light pulses of different wavelengths, and outputs are either absorbance or fluorescence at certain wavelengths. The various individual kinds of logic operations have been described previously, but each operation was realized in a different molecular system. The FG-DTE molecule unites and functionally integrates all these logic gates and circuits in a single molecular platform that can be addressed, read out, and reset photonically, implying a single initial state FGo-DTEo. The different responses of the two kinds of chromophores to any given input wavelength and the ability of the chromophores to influence one-another's properties via singlet energy transfer enable this flexibility of behavior, which is not shared by transistors or other more traditional logic devices. For example, the molecule can perform four simple logic functions in response to the same two inputs, depending upon the readout, and this allows complex functions such as addition, subtraction and demultiplexing. Some of the discussed functions can be realized in parallel by reading the optical responses in one absorption spectral scan, while others are conveniently accessible by reconfiguration through changing the input wavelength combinations and/or output reading. The initial state of the system can be reset from any point of operation by broadband green light irradiation and the stable recycling of the same operation is guaranteed by the reported high fatigue resistance of DTE and FG photochromes.<sup>11</sup> Although it is unlikely that such molecular devices will soon replace electronic computers, they could be readily applied in data storage<sup>27,28</sup> and where traditional computers cannot be used, such as micro-object labeling and tracking,<sup>26</sup> programmed drug release,<sup>22</sup> molecular self-regulation and control,<sup>60,61</sup> and related functions in nanotechnology and biomedicine. If molecular computing is realized in the future then the herein reported system with its unprecedented level of complexity represents a potential candidate as a highly versatile building block.<sup>62</sup>

## ASSOCIATED CONTENT

**Supporting Information.** Structures and absorption spectra of model monomers, isomerization kinetics, and detailed description of the input conditions. This material is available free of charge via the Internet at <http://pubs.acs.org>.

## AUTHOR INFORMATION

### Corresponding Author

a-son@chalmers.se; uwe.pischel@diq.uhu.es; gust@asu.edu

## ACKNOWLEDGMENT

This work was supported by a grant from the U.S. National Science Foundation (CHE-0846943), the Swedish Research Council (grant 622-2010-280), the European Research Council (grant ERC FP7/2007-2013 No. 203952), the Spanish Ministry of Science and Innovation (grant CTQ2008-06777-C02-02/BQU), and the Regional Ministry of Economy, Innovation, and Science of Andalusia (grant P08-FQM-3685).

## REFERENCES

- (1) de Silva, A. P.; Gunaratne, H. Q. N.; McCoy, C. P. *Nature* **1993**, *364*, 42–44.
- (2) de Silva, A. P.; Uchiyama, S. *Nat. Nanotechnol.* **2007**, *2*, 399–410.
- (3) Szacilowski, K. *Chem. Rev.* **2008**, *108*, 3481–3548.
- (4) Andréasson, J.; Pischel, U. *Chem. Soc. Rev.* **2010**, *39*, 174–188.
- (5) Margulies, D.; Melman, G.; Shanzer, A. *J. Am. Chem. Soc.* **2006**, *128*, 4865–4871.
- (6) Pischel, U. *Angew. Chem. Int. Ed.* **2007**, *46*, 4026–4040.
- (7) Bozdemir, O. A.; Guliyev, R.; Buyukcakil, O.; Selcuk, S.; Kolemen, S.; Gulseren, G.; Nalbantoglu, T.; Boyaci, H.; Akkaya, E. U. *J. Am. Chem. Soc.* **2010**, *132*, 8029–8036.
- (8) Andréasson, J.; Straight, S. D.; Bandyopadhyay, S.; Mitchell, R. H.; Moore, T. A.; Moore, A. L.; Gust, D. *Angew. Chem. Int. Ed.* **2007**, *46*, 958–961.
- (9) Amelia, M.; Baroncini, M.; Credi, A. *Angew. Chem. Int. Ed.* **2008**, *47*, 6240–6243.
- (10) Pérez-Inestrosa, E.; Montenegro, J.-M.; Collado, D.; Suau, R. *Chem. Commun.* **2008**, 1085–1087.
- (11) Andréasson, J.; Straight, S. D.; Moore, T. A.; Moore, A. L.; Gust, D. *J. Am. Chem. Soc.* **2008**, *130*, 11122–11128.
- (12) Ceroni, P.; Bergamini, G.; Balzani, V. *Angew. Chem. Int. Ed.* **2009**, *48*, 8516–8518.
- (13) Margulies, D.; Felder, C. E.; Melman, G.; Shanzer, A. *J. Am. Chem. Soc.* **2007**, *129*, 347–354.
- (14) Strack, G.; Ornatska, M.; Pita, M.; Katz, E. *J. Am. Chem. Soc.* **2008**, *130*, 4234–4235.
- (15) Sun, W.; Zhou, C.; Xu, C.-H.; Fang, C.-J.; Zhang, C.; Li, Z.-X.; Yan, C.-H. *Chem. Eur. J.* **2008**, *14*, 6342–6351.
- (16) Suresh, M.; Ghosh, A.; Das, A. *Chem. Commun.* **2008**, 3906–3908.
- (17) Andréasson, J.; Straight, S. D.; Moore, T. A.; Moore, A. L.; Gust, D. *Chem. Eur. J.* **2009**, *15*, 3936–3939.
- (18) Dilek, G.; Akkaya, E. U. *Tetrahedron Lett.* **2000**, *41*, 3721–3724.
- (19) Ferreira, R.; Remón, P.; Pischel, U. *J. Phys. Chem. C* **2009**, *113*, 5805–5811.
- (20) Credi, A. *Angew. Chem. Int. Ed.* **2007**, *46*, 5472–5475.
- (21) Magri, D. C.; Brown, G. J.; McClean, G. D.; de Silva, A. P. *J. Am. Chem. Soc.* **2006**, *128*, 4950–4951.
- (22) Amir, R. J.; Popkov, M.; Lerner, R. A.; Barbas, C. F., III; Shabat, D. *Angew. Chem. Int. Ed.* **2005**, *44*, 4378–4381.
- (23) Ozlem, S.; Akkaya, E. U. *J. Am. Chem. Soc.* **2009**, *131*, 48–49.
- (24) Konry, T.; Walt, D. R. *J. Am. Chem. Soc.* **2009**, *131*, 13232–13233.
- (25) Margulies, D.; Hamilton, A. D. *J. Am. Chem. Soc.* **2009**, *131*, 9142–9143.
- (26) de Silva, A. P.; James, M. R.; McKinney, B. O. F.; Pears, D. A.; Weir, S. M. *Nat. Mater.* **2006**, *5*, 787–790.
- (27) Irie, M. *Chem. Rev.* **2000**, *100*, 1685–1716.
- (28) Kärnbratt, J.; Hammerson, M.; Li, S.; Anderson, H. L.; Albinsson, B.; Andréasson, J. *Angew. Chem. Int. Ed.* **2010**, *49*, 1854–1857.

- (29) Gupta, T.; van der Boom, M. E. *Angew. Chem. Int. Ed.* **2008**, *47*, 5322–5326.
- (30) Motornov, M.; Zhou, J.; Pita, M.; Gopishetty, V.; Tokarev, I.; Katz, E.; Minko, S. *Nano Lett.* **2008**, *8*, 2993–2997.
- (31) Angelos, S.; Yang, Y.-W.; Khashab, N. M.; Stoddart, J. F.; Zink, J. I. *J. Am. Chem. Soc.* **2009**, *131*, 11344–11346.
- (32) Tokarev, I.; Gopishetty, V.; Zhou, J.; Pita, M.; Motornov, M.; Katz, E.; Minko, S. *ACS Appl. Mater. Interfaces* **2009**, *1*, 532–536.
- (33) Ball, P. *Nature* **2000**, *406*, 118–120.
- (34) Pischel, U. *Aust. J. Chem.* **2010**, *63*, 148–164.
- (35) Raymo, F. M.; Giordani, S. *Org. Lett.* **2001**, *3*, 1833–1836.
- (36) Raymo, F. M.; Giordani, S. *Org. Lett.* **2001**, *3*, 3475–3478.
- (37) Remacle, F.; Speiser, S.; Levine, R. D. *J. Phys. Chem. B* **2001**, *105*, 5589–5591.
- (38) Niazov, T.; Baron, R.; Katz, E.; Lioubashevski, O.; Willner, I. *Proc. Natl. Acad. Sci. U.S.A.* **2006**, *103*, 17160–17163.
- (39) Seelig, G.; Soloveichik, D.; Zhang, D. Y.; Winfree, E. *Science* **2006**, *314*, 1585–1588.
- (40) Frezza, B. M.; Cockroft, S. L.; Ghadiri, M. R. *J. Am. Chem. Soc.* **2007**, *129*, 14875–14879.
- (41) Silvi, S.; Constable, E. C.; Housecroft, C. E.; Beves, J. E.; Dunphy, E. L.; Tomasulo, M.; Raymo, F. M.; Credi, A. *Chem. Eur. J.* **2009**, *15*, 178–185.
- (42) Katz, E.; Privman, V. *Chem. Soc. Rev.* **2010**, *39*, 1835–1857.
- (43) de Silva, A. P.; Dixon, I. M.; Gunaratne, H. Q. N.; Gunnlauugsson, T.; Maxwell, P. R. S.; Rice, T. E. *J. Am. Chem. Soc.* **1999**, *121*, 1393–1394.
- (44) Gust, D.; Moore, T. A.; Moore, A. L. *Chem. Commun.* **2006**, 1169–1178.
- (45) de Silva, A. P.; Dobbin, C. M.; Vance, T. P.; Wannalser, B. *Chem. Commun.* **2009**, 1386–1388.
- (46) Pischel, U.; Uzunova, V. D.; Remón, P.; Nau, W. M. *Chem. Commun.* **2010**, *46*, 2635–2637.
- (47) de Silva, A. P. *Chem. Asian J.* **2011**, *6*, 750–766.
- (48) Raymo, F. M.; Giordani, S. *J. Am. Chem. Soc.* **2001**, *123*, 4651–4652.
- (49) Raymo, F. M. *Adv. Mater.* **2002**, *14*, 401–414.
- (50) Szaciłowski, K. *Chem. Eur. J.* **2004**, *10*, 2520–2528.
- (51) Margulies, D.; Melman, G.; Shanzer, A. *Nat. Mater.* **2005**, *4*, 768–771.
- (52) Baron, R.; Lioubashevski, O.; Katz, E.; Niazov, T.; Willner, I. *J. Phys. Chem. A* **2006**, *110*, 8548–8553.
- (53) Liu, Y.; Jiang, W.; Zhang, H.-Y.; Li, C.-J. *J. Phys. Chem. B* **2006**, *110*, 14231–14235.
- (54) Semeraro, M.; Credi, A. *J. Phys. Chem. C* **2010**, *114*, 3209–3214.
- (55) de Ruiter, G.; Tartakovsky, E.; Oded, N.; van der Boom, M. E. *Angew. Chem. Int. Ed.* **2010**, *49*, 169–172.
- (56) Pischel, U. *Angew. Chem. Int. Ed.* **2010**, *49*, 1356–1358.
- (57) Pischel, U.; Andréasson, J. *New J. Chem.* **2010**, *34*, 2701–2703.
- (58) Guo, Z.; Zhu, W.; Shen, L.; Tian, H. *Angew. Chem. Int. Ed.* **2007**, *46*, 5549–5553.
- (59) Remón, P.; Ferreira, R.; Montenegro, J.-M.; Suau, R.; Pérez-Inestrosa, E.; Pischel, U. *ChemPhysChem* **2009**, *10*, 2004–2007.
- (60) Straight, S. D.; Kodis, G.; Terazono, Y.; Hamburger, M.; Moore, T. A.; Moore, A. L.; Gust, D. *Nat. Nanotechnol.* **2008**, *3*, 280–283.
- (61) Keirstead, A. E.; Bridgewater, J. W.; Terazono, Y.; Kodis, G.; Straight, S.; Liddell, P. A.; Moore, A. L.; Moore, T. A.; Gust, D. *J. Am. Chem. Soc.* **2010**, *132*, 6588–6595.
- (62) Tian, H. *Angew. Chem. Int. Ed.* **2010**, *49*, 4710–4712.